

## Stability of Macroscopic Traffic Flow Modeling through Wavefront Expansion

Jingang Yi\*, Hao Lin\*, Luis Alvarez<sup>†</sup>, and Roberto Horowitz\*

\* *Department of Mechanical Engineering, University of California, Berkeley, CA 94720, USA*

<sup>†</sup> *Instituto de Ingeniería Universidad Nacional Autónoma de México, 04510 Coyoacán DF, México*

### Abstract

In this paper, the state of the art of macroscopic vehicle traffic flow models is discussed and the traffic flow stability of these models is analyzed. A nonlinear traffic flow stability criterion is investigated using the wavefront expansion technique. Qualitative relationships between traffic flow stability and model parameters are derived for an entire class of second-order macroscopic traffic flow models. Numerical results are obtained using the CLAWPACK package for the well-known Payne-Whitham (PW) model, in order to illustrate the stability criterion. The newly derived stability results are consistent with previous reported results obtained using both microscopic models and approximate linearization methods. Moreover, the stability criteria derived in this paper can provide more refined information regarding the propagation of traffic flow perturbations and shock waves in second-order models than previously established methodologies.

### 1 Introduction

Traffic flow stability is an important subject because congestion caused by an unstable traffic stream degrades the performance of road transportation networks. There is a large body of research that deals with the stability of traffic flow. [1] discussed traffic stability for various well-known microscopic traffic flow models, i.e. car following models. [2] presented a stability criterion for a well-known second-order macroscopic traffic flow model, known as Payne-Whitham (PW) model. [3] introduced a formal definition of traffic flow stability (based on the macroscopic traffic flow description) and related it to string stability (based on a car-following model). In [4], traffic stability analyses are presented for a new second-order continuum traffic model introduced in that paper and for the PW model. Most of these previous works are based on deterministic traffic models. Recently, [5] discussed the propagation of perturbations in dense traffic flow using a stochastic approximation approach and a microscopic model.

In this paper, we focus on the discussion of traffic propagation stability, namely, whether a traffic perturbation either forms a shock wave or decays to its equilibrium

state during its propagation along the highway. Moreover, we also analyze the relationship between the traffic propagation stability and the equilibrium traffic density and velocity for various second-order traffic models. To accomplish these goals, we apply a wavefront technique to traffic systems, which results in a generalized stability criterion that applies to an entire class of second-order models. This stability criterion is compared with the macroscopic model criteria given in [2] and other subsequent works for a few second-order models, and the conditions for stability or instability are shown to be consistent. The previous stability results are based on linearization methods for small magnitude perturbations, whereas the wavefront expansion technique presented in this paper accurately captures the nonlinear dynamics at the wavefront for large perturbations. Another valuable fact that we find in this study is that the magnitude of the moving downstream wave propagation, which was criticized by [6] as a major deficiency of most second-order models, decays quickly under certain conditions. Therefore, we believe that the effect of such a deficiency in some second-order models may not be significant, under a proper choice of model parameters. Some numerical examples illustrate this finding for the PW model.

This paper consists of six parts. In section 2, several different macroscopic traffic flow models are reviewed and a definition of stability of traffic flow is presented. Section 3 discusses the traffic flow characteristics. The stability results are presented in section 4. Section 5 presents some numerical examples to illustrate the stability results in section 4. Concluding remarks are presented in section 6.

### 2 Macroscopic Traffic Flow Models and Stability

In the past 50 years, a significant amount of research has been done on macroscopic modeling of traffic flows. In this paper we consider only a one lane highway without any on- or off-ramps.<sup>1</sup> Let  $\rho(x, t)$  denote the highway density,  $q(x, t)$  the flow and  $v(x, t)$  the traffic velocity at position  $x$  along the highway at time  $t$ , respectively.

<sup>1</sup>We can drop this assumption by adding relaxation terms in the conservation laws.

Note that the traffic velocity  $v(x, t)$  is the average speed of all individual vehicles on the highway around  $x$  [7]. Conservation of vehicles on the highway gives us the following equation <sup>2</sup>:

$$\frac{\partial \rho}{\partial t} + \frac{\partial(\rho v)}{\partial x} = 0 \quad (1)$$

and the velocity dynamics for various models can be written, in a general form, as

$$\frac{\partial v}{\partial t} + v \frac{\partial v}{\partial x} = -\frac{1}{\rho} \frac{\partial \mathcal{P}}{\partial x} + \frac{1}{\tau} (V_e - v) \quad (2)$$

where  $V_e$  is the generalized equilibrium velocity given by the fundamental diagram relationship between highway velocity  $v$  and density  $\rho$ ,  $\mathcal{P}$  is the so-called traffic pressure, and  $\tau$  is the so-called relaxation time.

For various macroscopic models, the traffic pressure  $\mathcal{P} := \mathcal{P}(\rho, v)$ , relaxation time  $\tau$ , and the generalized equilibrium velocity  $V_e(\rho, v)$  <sup>3</sup> are different:

1. If  $\tau = 0$ ,  $\mathcal{P} = 0$ , we obtain the LWR first order model [8] and [9].
2. If  $\mathcal{P} = -\frac{V_e(\rho)}{2\tau}$  with  $V_e(\rho, v) = V_e(\rho)$ , we obtain the PW model.
3. Setting  $\mathcal{P} = \rho\Theta$  with  $\Theta = \Theta_0(1 - \frac{\rho}{\rho_{max}})$  results in the model given in [10].
4. If  $\mathcal{P} = \frac{\nu}{\gamma+2}\rho^{\gamma+2}$ , where  $\nu$  is an anticipation parameter and  $\gamma$  a dimensionless constant; and  $V_e(\rho) = V_f$ , where  $V_f$  is the free flow velocity; we obtain the model given in [11]. A similar model to that of [12] is obtained for  $\mathcal{P} = \frac{1}{3}\rho^3 V_e'(\rho)$  <sup>4</sup> with  $V_e'(\rho) = \frac{dV_e(\rho)}{d\rho}$ .

Each of these models has been tested either in simulation or against real traffic flow measurements. In this paper, we are not going to discuss which model is the most accurate to fit real traffic measurements. Instead, we focus on studying the stability properties of these second-order models under perturbed initial conditions, assuming dense traffic flow. Since the second-order traffic models have been widely used for traffic flow studies for various purposes, we believe that a systematic investigation of stability for those models is valuable to

<sup>2</sup>In this paper we assume that the traffic flow variables  $\rho(x, t)$ ,  $q(x, t)$  and  $v(x, t)$  are differentiable.

<sup>3</sup>For most high order traffic flow models,  $V_e$  is only a function of density  $\rho$ , i.e.  $V_e(\rho, v) = V_e(\rho)$ . However, here we extend this assumption, and consider  $V_e(\rho, v)$  to be a function of both density  $\rho$  and flow velocity  $v$ , in order to accommodate various models.

<sup>4</sup>In this paper, for simplicity, we consider  $V_e(\rho)$  to be piecewise linear for Zhang's model, thus  $V_e''(\rho) = 0$ . If other complicated functions are used for the fundamental diagram, the results are similar but more difficult to compute.

better understand their intrinsic properties. A few linear stability results have been reported for some specific second-order traffic models, such as the PW and Zhang's models [2, 4]. However, there is no uniform nonlinear study of a general second-order traffic model. This paper fills this gap.

First, we should define the stability of the systems described by Eqs. (1) and (2). Let  $\mathbf{q} = [\rho, v]^T$  and let  $d(\mathbf{q}, t) : \mathbb{R}_+^2 \times \mathbb{R}_+ \mapsto \mathbb{R}_+$ , where  $\mathbb{R}_+ = [0, \infty)$ , be a spatial metric. For example, we can take  $d(\mathbf{q}; t) = \sup_x \|\mathbf{q}(x, t)\|$ . We can use the stability definition of continuous systems from [13], and extend it to the traffic flow system of Eqs. (1) and (2).

**Definition 1 (Traffic flow stability)** Let  $\mathbf{q}_e(x, t) = [\rho_e(x, t), v_e(x, t)]^T$  denote the nominal equilibrium state of the traffic. Let  $\mathbf{q}_p$  be the perturbed states. The traffic state  $\mathbf{q}_e$  is stable, if for every  $\epsilon > 0$ , there is  $\delta > 0$  such that for every perturbed state  $\mathbf{q}_p$  which satisfies, at the initial instant  $t_0$  and  $x_0$ , the condition

$$d(\mathbf{q}_p - \mathbf{q}_e; t_0) < \delta$$

it is true that

$$d(\mathbf{q}_p - \mathbf{q}_e; t) < \epsilon$$

for all  $t \geq t_0$ . If, in addition to the above,  $\lim_{t \rightarrow \infty} d(\mathbf{q}_p - \mathbf{q}_e; t) = 0$ , then, the traffic state  $\mathbf{q}_e$  is asymptotically stable.

In this paper, we mainly focus on the following definition of traffic flow propagation stability.

**Definition 2 (Traffic flow propagation stability)** Let  $\mathbf{q}_e(x, t) = [\rho_e(x, t), v_e(x, t)]^T$  denote the nominal equilibrium state of the traffic. The traffic flow  $\mathbf{q}_e$  is propagation stable if the system does not generate any shock wave along the wavefront for every perturbed traffic state  $\mathbf{q}_p$ .

The wavefront of a traffic system can be illustrated by Fig. 1. Consider a pair of equilibrium states,  $\mathbf{q}_e = [\rho_e, v_e]$ , of the traffic system, if there is a perturbation at position  $x_0$ , then the wavefront is the propagation curve of such perturbation along the unperturbed density and velocity. If a traffic system is propagation stable, then the magnitude of the initial perturbation should not increase during its propagations. On the other hand, if a traffic system is propagation unstable, a perturbed density or velocity could then propagate increasingly and finally form a shock wave or bottleneck on the highway. In this paper, we focus on how a perturbed density or velocity profile propagates if we use a second-order model to study traffic behaviors.

In this paper we prefer to use the definition of the traffic propagation stability instead of other definitions of stability like the one in [3] because normally transportation engineers refer to traffic instability to the formation of a shock wave, which is the propagation stability defined in this paper. In the rest of this paper, we will refer to traffic stability as traffic propagation stability.

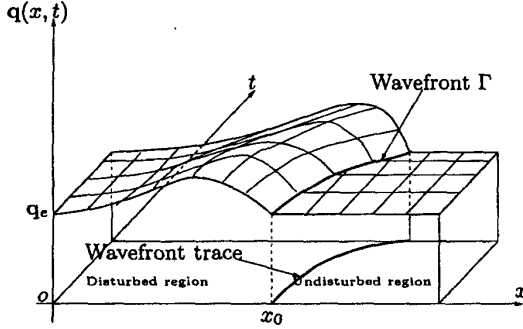


**Figure 1:** A schematic of a solution surface, wavefront and wavefront trace with an initial  $C^1$  discontinuous condition  $q(x_0, 0)$ .

It is important to distinguish between small and large perturbations in the stability analysis of traffic systems (see Fig. 2). Most transportation researchers have used linearized methods to analyze traffic stability by assuming that the perturbations are small. For example, [2], [3] and [4]. The approximate linearization stability analysis of the nonlinear PDE system (1) and (2) is only valid when the magnitude of the perturbations is small, since the analysis neglects higher order terms. However, when the perturbation is fairly large, the linearization method may produce incorrect results as pointed out by [2]. Therefore, it is necessary to use other techniques to analyze traffic stability under large perturbations. In this paper, we discuss one of such approaches by utilizing a wavefront expansion technique.

### 3 Traffic Flow Characteristics

To discuss traffic flow stability we need to first investigate the characteristic velocity of a traffic system given by Eqs. (1) and (2). From now on, we use shortened notation to denote partial derivatives, for example,  $\rho_x := \frac{\partial \rho}{\partial x}$ . We also assume that the traffic pressure function  $\mathcal{P}(\rho, v) : \mathbb{R}_+ \times \mathbb{R}_+ \mapsto \mathbb{R}$  is smooth, i.e.  $\mathcal{P} := \mathcal{P}(\rho, v) \in C^\infty(\mathbb{R}_+ \times \mathbb{R}_+)$ . We thus rewrite Eq. (1) as

$$\rho_t + v\rho_x + \rho v_x = 0 \quad (3)$$

and, using the fact  $\mathcal{P} = \mathcal{P}(\rho, v)$ , rewrite Eq. (2) as

$$v_t + \frac{1}{\rho}\mathcal{P}_\rho\rho_x + \left(v + \frac{1}{\rho}\mathcal{P}_v\right)v_x = \frac{1}{\tau}(V_e - v). \quad (4)$$

Consider the full differentials of  $\rho(x, t)$  and  $v(x, t)$  as follows

$$d\rho(x, t) = \rho_x dx + \rho_t dt \quad (5)$$

$$dv(x, t) = v_x dx + v_t dt \quad (6)$$

and write Eqs. (3) – (6) in matrix form

$$\begin{bmatrix} 1 & v & 0 & \rho \\ 0 & \frac{1}{\rho}\mathcal{P}_\rho & 1 & \left(v + \frac{1}{\rho}\mathcal{P}_v\right) \\ dt & dx & 0 & 0 \\ 0 & 0 & dt & dx \end{bmatrix} \begin{bmatrix} \rho_t \\ \rho_x \\ v_t \\ v_x \end{bmatrix} = \begin{bmatrix} 0 \\ \frac{1}{\tau}(V_e - v) \\ d\rho \\ dv \end{bmatrix}.$$

To admit discontinuous solutions (shocks) for  $\rho(x, t)$  and  $v(x, t)$ , which are observed in real traffic flow, it is necessary that the coefficient matrix be singular. Therefore, the characteristic velocities  $v_c$  are given by

$$v_c := \frac{dx}{dt} = v + \frac{1}{2\rho}\mathcal{P}_v \pm \sqrt{\frac{1}{4\rho^2}(\mathcal{P}_v)^2 + \mathcal{P}_\rho}. \quad (7)$$

For each of the different models discussed above, the characteristic velocities have the following formulae:

1. For the PW model,  $\mathcal{P} = -\frac{V_e(\rho)}{2\tau}$ , then from Eq. (7),

$$v_c = v \pm \sqrt{-\frac{1}{2\tau} \frac{\partial V_e}{\partial \rho}}.$$

2. For Phillips's model,  $\mathcal{P} = \Theta_0 \rho \left(1 - \frac{\rho}{\rho_{max}}\right)$  and

$$v_c = v \pm \sqrt{\Theta_0 \left(1 - \frac{2\rho}{\rho_{max}}\right)}.$$

3. For Michalopoulos' model  $\mathcal{P} = \frac{\nu}{\gamma+2}\rho^{\gamma+2}$  and

$$v_c = v \pm \sqrt{\nu\rho^{\gamma+1}},$$

and, for Zhang's model,  $\mathcal{P} = \frac{1}{3}\rho^3 V_e'(\rho)$  and

$$v_c = v \pm |V_e'(\rho)|\rho.$$

**Remark 1** From the above calculations we find that, for all the second-order traffic flow models considered in this paper, one of the solutions of the characteristic velocity is larger than the average traffic flow velocity  $v$ . This is not realistic, since shock waves do not propagate to the downstream traffic in actual highways, and this fact has been criticized by [6] and [14] as a major deficiency of most second-order models. Several researchers, such as [15], have proposed some modified second-order models in which all characteristic velocities are smaller than vehicle traveling velocity. However, such modifications are limited to some specific situations and the

resulting modified models lack physical interpretations. From Eq. (7), the characteristic velocity  $v_c \leq v$  iff

$$\mathcal{P}_v \leq 0, \mathcal{P}_\rho \leq 0, \text{ and } \frac{1}{4\rho^2} \mathcal{P}_v^2 + \mathcal{P}_\rho \geq 0. \quad (8)$$

Even though there is such a major deficiency as discussed above, we investigate the stability conditions for the various second-order traffic models in this paper because, most second-order models have been applied to either simulation tests or real traffic measurements and have been validated to capture some important properties of traffic systems. More importantly, in this paper we find that, for most second-order traffic models, the perturbation that travels faster than traffic decays quickly. Numerical examples in section 5 illustrate this fact. Therefore, we believe that the effect of such a deficiency in some second-order models may not be significant under proper tuning of the model parameters.

#### 4 Stability Results

In this section we discuss the propagation stability conditions for second-order traffic flow models (Eqs. (1) and (2)) under large perturbations. Here we consider a fairly large perturbation around the equilibrium density  $\rho_e$  and average velocity  $V_e$ . Fig. 2 shows a schematic of such a perturbation versus small perturbations. Suppose that traffic has a constant traffic density  $\rho_0 = \rho_e$  and velocity  $v_0 = V_e(\rho_e)$ , where the  $(\rho_e, V_e(\rho_e))$  pair is on the fundamental diagram. Obviously,  $\rho_0, v_0$  are the solutions of Eqs. (1) and (2). Assume a disturbance, such as a ‘‘bump’’ in Fig. 2, around the density  $\rho_0$  and its corresponding equilibrium velocity  $v_0$ . Without loss of generality, assume that the first derivative of the density profile around the wavefront  $P$  is discontinuous<sup>5</sup>.

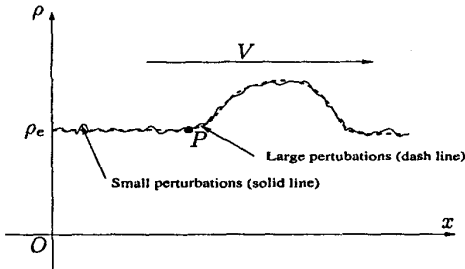


**Figure 2:** A schematic of perturbed traffic density profile

It is particularly convenient to expand the solution of the system around the wavefront in powers of

$$\zeta = x - X(t), \quad (9)$$

<sup>5</sup>This assumption can be generalized. For example, if the  $m$ th derivatives of  $\rho$  and  $v$  are the first ones to be discontinuous, the expanded power series (Eqs. (11) and (12)) beyond  $\rho_0$  and  $v_0$  start with the term in  $\zeta^m$ .

where the wavefront has the characteristic velocity  $v_c$  at the equilibrium states, i.e.

$$\dot{X}(t) = v_0 + u_0 = v_0 + \frac{1}{2\rho_0} \mathcal{P}_v^0 \pm \sqrt{\frac{1}{4\rho_0^2} (\mathcal{P}_v^0)^2 + \mathcal{P}_\rho^0} \quad (10)$$

$$\text{and } u_0 := \frac{1}{2\rho_0} \mathcal{P}_v^0 \pm \sqrt{\frac{1}{4\rho_0^2} (\mathcal{P}_v^0)^2 + \mathcal{P}_\rho^0}, \mathcal{P}_v^0 = \mathcal{P}_v \Big|_{(\rho_0, v_0)}$$

$$\text{and } \mathcal{P}_\rho^0 = \mathcal{P}_\rho \Big|_{(\rho_0, v_0)}.$$

Using Eq. (9), we can expand the flow variables  $\rho$  and  $v$  behind the wavefront in a power series of  $\zeta$  as

$$\rho(x, t) = \rho_0 + \zeta \rho_1(t) + \frac{1}{2} \zeta^2 \rho_2(t) + \dots \quad (11)$$

$$v(x, t) = v_0 + \zeta v_1(t) + \frac{1}{2} \zeta^2 v_2(t) + \dots, \quad (12)$$

where

$$\rho_i(t) = \frac{\partial^i \rho}{\partial x^i} \Big|_{(X(t)-, t)}, \quad v_i(t) = \frac{\partial^i v}{\partial x^i} \Big|_{(X(t)-, t)}, \quad i = 1, 2, 3, \dots$$

Using Eqs. (11) and (12), we obtain

$$\rho_t = -\dot{X}(t) \rho_1(t) + \zeta \dot{\rho}_1(t) - \zeta \dot{X}(t) \rho_2(t) + \dots \quad (13a)$$

$$\rho_x = \rho_1(t) + \zeta \rho_2(t) + \frac{1}{2} \zeta^2 \rho_3(t) + \dots \quad (13b)$$

$$v_t = -\dot{X}(t) v_1(t) + \zeta \dot{v}_1(t) - \zeta \dot{X}(t) v_2(t) + \dots \quad (13c)$$

$$v_x = v_1(t) + \zeta v_2(t) + \frac{1}{2} \zeta^2 v_3(t) + \dots \quad (13d)$$

Similarly, for  $\mathcal{P}$  and  $V_e(\rho)$ , we obtain

$$\mathcal{P}_v = \mathcal{P}_v^0 + \zeta [\mathcal{P}_{v\rho}^0 \rho_1(t) + \mathcal{P}_{vv}^0 v_1(t)] + \dots \quad (14a)$$

$$\mathcal{P}_\rho = \mathcal{P}_\rho^0 + \zeta [\mathcal{P}_{\rho\rho}^0 \rho_1(t) + \mathcal{P}_{\rho v}^0 v_1(t)] + \dots \quad (14b)$$

$$V_e(\rho, v) = V_e^0 + \zeta [(V_e)_\rho^0 \rho_1(t) + (V_e)_v^0 v_1(t)] + \dots, \quad (14c)$$

where  $V_e^0 := V_e(\rho_0)$ ,  $(V_e)_\rho^0 := \frac{\partial V_e}{\partial \rho} \Big|_{(\rho_0, v_0)}$  and  $(V_e)_v^0 := \frac{\partial V_e}{\partial v} \Big|_{(\rho_0, v_0)}$ .

Substituting Eqs. (13) and (14) into Eq. (2), for the coefficients of the first two terms  $\zeta^0$  and  $\zeta^1$ , we obtain

$$\dot{\rho}_1 - \rho_2 u_0 + 2\rho_1 v_1 + \rho_0 v_2 = 0 \quad (15a)$$

$$\rho_0 \dot{\rho}_1 + v_2 (\mathcal{P}_v^0 - \rho_0 u_0) + \rho_2 \mathcal{P}_\rho^0 + \rho_1 v_1 (2\mathcal{P}_{\rho v}^0 - u_0) + v_1^2 (\rho_0 + \mathcal{P}_{vv}^0) + \rho_1^2 \mathcal{P}_{\rho\rho}^0 + \frac{1}{\tau} [v_1 - (V_e)_\rho^0 \rho_1 - (V_e)_v^0 v_1] = 0. \quad (15b)$$

For Eqs. (15a) and (15b), we obtain

$$\dot{v}_1 + \alpha v_1 + \beta v_1^2 = 0, \quad (16)$$

where

$$\alpha = \frac{\rho_0 u_0}{\tau(2\rho_0 u_0 - \mathcal{P}_v^0)} \left( 1 - (V_e)_v^0 - \frac{(V_e)_\rho^0 \rho_0}{u_0} \right),$$

$$\beta = \frac{\left( \rho_0 \frac{\partial}{\partial \rho} + u_0 \frac{\partial}{\partial v} \right)^2 \mathcal{P}^0 + 2\rho_0 \mathcal{P}_\rho^0}{u_0(2\rho_0 u_0 - \mathcal{P}_v^0)}.$$

Notice that  $v_1(t) = \frac{\partial v(x,t)}{\partial x} \Big|_{(X(t), t)}$ , namely, the slope of the wavefront at point  $P$ . The above Riccati equation gives the slope evolution at the wavefront. The propagation stability of Eq. (16) can thus be analyzed in terms of the initial condition  $v_1(0)$  and the parameters  $\alpha$  and  $\beta$ . Table 1 shows the stability conditions of the system given by Eq. (16). Moreover, the solution of the Riccati equation (16) is given as

$$v_1(t) = \frac{\alpha}{\beta} \frac{e^{-\alpha t}}{\left( 1 + \frac{\alpha}{\beta v_1(0)} \right) - e^{-\alpha t}}, \quad (17)$$

where  $v_1(0)$  is the initial condition for  $v_1(t)$  at  $t = 0$ .

For the second-order traffic flow models that were discussed in section 2, we can use the above results to calculate the stability criterion for various models. There are two different characteristic velocities for second-order traffic models: one moving downstream at speed  $v_0 + u_{01}$  ( $> v_0$ ) and another moving upstream at speed  $v_0 + u_{02}$  ( $< v_0$ ), where  $u_{01}$  and  $u_{02}$  are two values of  $u_0$  given by Eq. (10). Notice that, for the moving downstream characteristic velocity  $v_c = v_0 + u_{01}$  with  $u_{01} > 0$ , and for most second-order traffic models,  $\mathcal{P}_v^0 = 0$ ,  $(V_e)_v^0 = 0$  and  $(V_e)_\rho^0 < 0$ , thus,

$$\alpha = \frac{1}{2\tau} \left( 1 + \frac{|(V_e)_\rho^0| \rho_0}{u_0} \right) \gg 1, \quad \beta > 0.$$

The magnitude of a perturbation moving downstream at characteristic speed  $v_0 + u_{01}$  therefore decays to zero quickly since  $v_1(t) \rightarrow 0$  quickly by the solution (17) for  $v_1(0) \geq -\frac{\alpha}{\beta}$ . We can thus neglect the effects of the forward moving branch of the perturbation for most second-order traffic models though these perturbations do not take place in actual traffic.

In the following, we consider the solution branch for which the characteristic velocity  $v_0 + u_{02}$  satisfies  $u_{02} < 0$ , i.e. the upstream moving branch.

For the PW model,  $\mathcal{P} = -\frac{V_e(\rho)}{2\tau}$ ,  $u_{02} = -\sqrt{-\frac{V_e'(\rho_0)}{2\tau}}$ , and

$$\alpha = \frac{1}{2\tau} \left( 1 - \rho_0 \sqrt{-2V_e'(\rho_0)\tau} \right), \quad \beta = 1.$$

Thus, for traffic flow perturbations, from Table 1, in order to have stability for any initial condition  $v_1(0) >$

**Table 1:** Stability conditions for system Eq. (16)

Parameters $\alpha$ and $\beta$	Stable region
$\beta > 0, \alpha > 0$	$v_1(0) \in [-\frac{\alpha}{\beta}, \infty), v_1(t) \rightarrow 0$
$\beta > 0, \alpha = 0$	$v_1(0) \in \mathbb{R}, v_1(t) \rightarrow 0$
$\beta > 0, \alpha < 0$	$v_1(0) \in [0, \infty), v_1(t) \rightarrow -\frac{\alpha}{\beta}$
$\beta < 0, \alpha = 0$	$\emptyset$
$\beta < 0, \alpha > 0$	$v_1(0) \in (-\infty, -\frac{\alpha}{\beta}), v_1(t) \rightarrow 0$
$\beta < 0, \alpha < 0$	$v_1(0) \in (-\infty, 0), v_1(t) \rightarrow -\frac{\alpha}{\beta}$
$\beta = 0, \alpha > 0$	$v_1(0) \in \mathbb{R}, v_1(t) \rightarrow 0$
$\beta = 0, \alpha < 0$	$\emptyset$

$-\frac{\alpha}{\beta}$ , we need  $\alpha \geq 0$ . Therefore we obtain

$$1 - \rho_0 \sqrt{-2V_e'(\rho_0)\tau} \geq 0,$$

which can be rearranged as

$$\frac{1}{2} \geq -\rho_0^2 V_e'(\rho_0)\tau. \quad (18)$$

The ‘‘negative’’ sign in the above inequality arises because  $V_e'(\rho) \leq 0$ . Condition (18) is the same as given in [2] and [1]. However, in [2] and [1], the stability conditions were derived using an approximate linearized stability analysis, and a microscopic traffic model, i.e. a car-following model, respectively.

For Philips’s model,  $\mathcal{P} = \rho\Theta \left( 1 - \frac{\rho}{\rho_{max}} \right)$ ,  $u_{02} = -\sqrt{\Theta_0 \left( 1 - \frac{2\rho}{\rho_{max}} \right)}$ . Assume that  $\rho_0 \leq \rho_{max}/3$ , then  $\beta \geq 0$ . In order to have stability for any initial condition  $v_1(0) > -\frac{\alpha}{\beta}$ , we need  $\alpha \geq 0$ , therefore the stability condition is

$$\rho_0 \leq \sqrt{\Theta_0 + \left( \frac{\Theta_0}{\rho_{max} V_e'^2(\rho_0)} \right)^2} - \frac{\Theta_0}{\rho_{max} V_e'^2(\rho_0)}. \quad (19)$$

For Michalopoulos’ model,  $\mathcal{P} = \frac{\nu}{\gamma+2} \rho^{\gamma+2}$ ,  $u_{02} = -\sqrt{\nu \rho^{\gamma+1}}$ . Noticing that  $V_e = V_f$  is independent of  $\rho$  and  $v$ , we have

$$\alpha = \frac{1}{2\tau}, \quad \beta = \frac{\gamma+3}{2}. \quad (20)$$

Thus, for any initial conditions  $v_1(0) > -\frac{\alpha}{\beta}$ , the system is stable. For Zhang’s model,  $\mathcal{P} = \frac{1}{3} \rho^3 V_e'^2$ ,  $u_{02} = -|V_e'(\rho)|\rho$  and

$$\alpha = \frac{1}{\tau}, \quad \beta = 2.$$

Since  $\beta > 0$ ,  $\alpha > 0$ , the slope of the perturbations around the wavefront converges to zero for  $v_1(0) > -\frac{\alpha}{\beta}$ ,

according to Table 1. This result is similar to the stability criterion found in [4]. In [4] the author claimed that the new model was “inherently stable, as is the LWR model, in the sense that the magnitude of a small disturbance in the traffic stream does not grow without a bound”. A linearized approximation was used to find the stability result in [4]. However, the stability results that were derived in this section for Zhang’s model are more precise since the slope magnitude of the disturbance does asymptotically converge to zero.

## 5 Numerical Examples

In this section we illustrate the results of the previous section with some numerical examples. Computing numerical solutions for conservation equations such as Eqs. (1) and (2) is difficult because of the subtlety of capturing discontinuous solutions such as shock waves. Recently, accurate numerical methods for conservation laws have been developed. CLAWPACK is based on the wave propagation algorithms, which is one of these methods [16]. Rewriting the macroscopic traffic model (1) and (2) in a conservation form as follows

$$\begin{bmatrix} \rho \\ \rho v \end{bmatrix}_t + \begin{bmatrix} \rho v \\ \rho v^2 + \mathcal{P} \end{bmatrix}_x = \begin{bmatrix} 0 \\ \frac{\rho}{\tau}(V_e - v) \end{bmatrix}, \quad (21)$$

and denoting  $\mathbf{p} = [\rho \quad \rho v]^T \in \mathbb{R}^2$ ,  $\mathbf{f}(\mathbf{p}) = [\rho v \quad \rho v^2 + \mathcal{P}]^T \in \mathbb{R}^2$  and  $\psi(\mathbf{p}) = [0 \quad \frac{\rho}{\tau}(V_e - v)]^T \in \mathbb{R}^2$ , Eq. (21) can be rewritten as

$$\mathbf{p}_t + \mathbf{f}(\mathbf{p})_x = \psi(\mathbf{p}), \quad (22)$$

which is in the form that can be solved directly by the wave propagation algorithms.

In what follows, we apply this numerical scheme to the PW model. For the PW model, the parameters and fundamental diagram are taken as [17]:  $\tau = 25$  sec.,  $\mu = \sqrt{-\frac{V_e'(\rho)}{2\tau}} = 56$  km/h, and  $V_e(\rho) = \min \left\{ 88.5, 88.5 \left[ 1.94 - 6 \left( \frac{\rho}{143} \right) + 8 \left( \frac{\rho}{143} \right)^2 - 3.93 \left( \frac{\rho}{143} \right)^3 \right] \right\}$  veh/km/lane.

In order to test the traffic flow stability condition that was obtained in the previous section, we need to first check the stability criterion (18). Since  $\mu = \sqrt{-\frac{V_e'(\rho)}{2\tau}} =$  constant, we need to modify the stability criterion (18) as follows:

$$1 + \frac{V_e'(\rho_0)\rho_0}{\mu} \geq 0.$$

We can compute the critical density  $\rho_c$  by solving the above algebraic equation, with  $0 \leq \rho_0 \leq 26$  veh/km/lane, or  $52.4 \leq \rho_0 \leq 114.7$  veh/km/lane,  $\rho_0 \in$

$[0, \rho_{max}]$ , where  $\rho_{max} = 143$  veh/km/lane is given by the PW model. Note that the critical density given by the PW fundamental diagram is  $\rho_c = 30$  veh/km/lane and that the characteristic velocity is  $v_c = v_0 \pm \mu$  and  $\mu = 56$  km/h (equivalently  $\rho = 51.5$  veh/km/lane). In order to guarantee that the perturbation waves propagate backwards, the stability region for the equilibrium density is given by  $52.4 \leq \rho_0 \leq 114.7$  veh/km/lane,  $\rho_0 \in [0, \rho_{max}]$ .

We design the following steady-state density profile as an initial condition to test the above results.

$$\rho(x, 0) = \begin{cases} \rho_0 + \Delta\rho \cos\left(\frac{\pi(x-x_0)}{2\Delta x}\right) & x \in [x_0 - \Delta x, x_0 + \Delta x] \\ \rho_0 & \text{other } x \in [0, L] \end{cases} \quad (23)$$

where  $L = 15$  km is the length of the highway. In our computations, we assume that the highway is long enough so that we do not need to feed the specific boundary conditions, and zero order extrapolation is used instead <sup>6</sup>.

The first scenario is a simulation of a stable situation. We choose the following initial conditions in Eq. (23):  $\rho_0 = 75$  veh/km/lane,  $\Delta\rho = 10$  veh/km/lane,  $x_0 = 10$  km,  $\Delta x = 0.5$  km and the numerical results are given in Fig. 3.

The second scenario is a test for the unstable situation. We choose the following initial conditions in Eq. (23):  $\rho_0 = 115$  veh/km/lane,  $\Delta\rho = 10$  veh/km/lane,  $x_0 = 10$  km,  $\Delta x = 0.5$  km and the numerical results are given in Fig. 4.

From above two examples, we observe that there are two perturbed waves generated by the initial conditions: one is moving forwards and the other backwards. The magnitude of the forward wave is much smaller than that of the backward wave. Moreover, the forward wave disappears quickly and the backward wave does not.

## 6 Conclusions

In this paper we discussed the traffic flow propagation stability using a nonlinear stability analysis technique. A generalized macroscopic traffic model was used for nonlinear stability analysis through the wavefront expansion method. A generalized stability criterion for macroscopic stability was proposed. For various macroscopic models we calculated the stability conditions and compared them with those that were obtained through linearized analysis by previous authors. We found that the proposed stability analysis yields the same conditions as previously obtained results, in the case where

<sup>6</sup>We can apply other boundary conditions. However, in this paper, we only test the stability criterion.

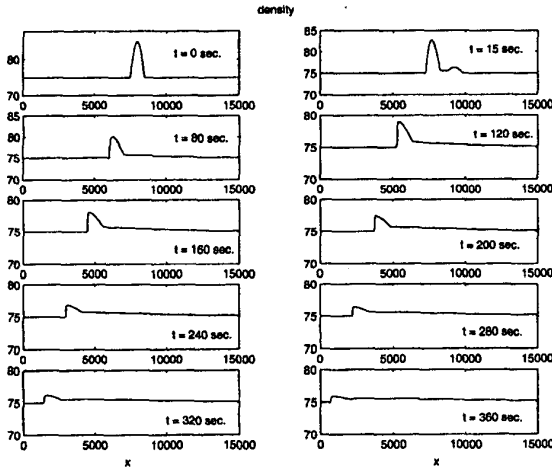


Figure 3: Time snapshot of density  $\rho$  for PW model (stable).

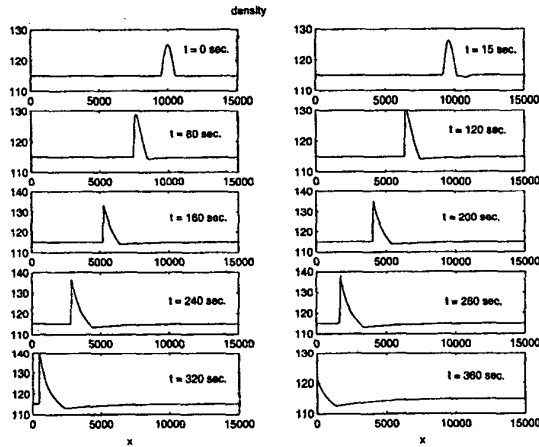


Figure 4: Time snapshot of density  $\rho$  for PW model (unstable).

such results existed. However, the nonlinear stability analysis in this paper gives more precise local stability information along the perturbation propagations than the approximate linear stability approach of previous approaches. Moreover, stability conditions were obtained for some models, which were not previously analyzed using linearization techniques. Some numerical examples have been presented to validate the theoretical results. The stability condition found in this paper can be further used for prediction of traffic stability and to perform a qualitative analysis of the relationships between traffic behaviors and traffic model parameters and structures.

#### References

[1] E. N. Holland, "A Generalized Stability Criterion for Motorway Traffic," *Transportation Research - B*, vol. 32, no.

2, pp. 141-154, 1998.

[2] G. B. Whitham, *Linear and Nonlinear Waves*, John Wiley and Sons Inc, New York, NY, 1974.

[3] D. Swaroop and K. R. Rajagopal, "Intelligent Cruise Control Systems and Traffic Flow Stability," *Transportation Research - C*, vol. 7, no. 6, pp. 329-352, 1999.

[4] H. M. Zhang, "Analyses of the Stability and Wave Properties of a New Continuum Traffic Theory," *Transportation Research - B*, vol. 33, no. 6, pp. 399-415, 1999.

[5] J. M. del Castillo, "Propagation of Perturbations in Dense Traffic Flow: A Model and Its Implications," *Transportation Research - B*, vol. 35, no. 4, pp. 367-389, 2001.

[6] Carlos F. Daganzo, "Requiem For Second-order Fluid Approximations of Traffic Flow," *Transportation Research - B*, vol. 29, no. 4, pp. 277-286, 1995.

[7] Markos Papageorgiou, "Some Remarks on Macroscopic Traffic Flow Modelling," *Transportation Research - B*, vol. 32, no. 5, pp. 323-329, 1998.

[8] M. J. Lighthill and J. B. Whitham, "On Kinematic Waves II: A Theory of Traffic Flow on Long Crowded Roads," in *Proceedings of the Royal Society*, 1955, vol. A229, pp. 317-345.

[9] Paul I. Richard, "Shock Waves on the Highway," *Operations Research*, vol. 4, pp. 42-51, 1956.

[10] Warren F. Phillips, "A Kinetic Model for Traffic Flow with Continuum Implications," *Transportation Planning and Technology*, vol. 5, pp. 131-138, 1979.

[11] Panos G. Michalopoulos, Ping Yi, and Anastasios S. Lyrintzis, "Continuum Modelling of Traffic Dynamics for Congested Freeways," *Transportation Research - B*, vol. 27, no. 4, pp. 315-332, 1993.

[12] H. M. Zhang, "A Theory of Nonequilibrium Traffic Flow," *Transportation Research - B*, vol. 32, no. 7, pp. 485-498, 1998.

[13] A. A. Movchan, "Stability of Processes With Respect to Two Metrics," *Applied Mathematical Mechanics*, vol. 24, no. 6, pp. 988-1001, 1960.

[14] Guoqiang Liu, Anastasios S. Lyrintzis, and Panos G. Michalopoulos, "Improved High-Order Model for Freeway Traffic Flow," *Transportation Research Board*, vol. 1644, pp. 37-46, 1998.

[15] J. M. del Castillo, P. Pintado, and F. G. Benítez, "A Formulation for the Reaction Time of Traffic Flow Models," *Transportation Research - B*, vol. 28, no. 1, pp. 35-60, 1994.

[16] Randall J. LeVeque, *CLAWPACK Version 4.0 User's Guide*, University of Washington, also <http://www.amath.washington.edu/~claw>, Seattle, WA, 2000.

[17] Harold J. Payne, "FREELO: a Macroscopic Simulation Model of Freeway Traffic," *Transportation Research Record*, vol. 772, pp. 68-75, 1979.